ELSEVIER

Chemical Engineering Journal 139 (2008) 213–223

Chemical Engineering Journal

www.elsevier.com/locate/cej

# Adsorption kinetics and mechanism of maxilon blue 5G dye on sepiolite from aqueous solutions

M. Alkan, M. Doğan*, Y. Turhan, Ö. Demirbaş, P. Turan

*Balikesir University, Faculty of Science and Literature, Department of Chemistry,*
*10145 Cagis/Balikesir, Turkey*

Received 19 March 2007; received in revised form 31 May 2007; accepted 24 July 2007

## Abstract

The use of sepiolite for the removal of maxilon blue 5G from aqueous solutions at different contact times, stirring speeds, initial dye concentrations, pHs, ionic strengths and temperatures was investigated. The adsorption process attained equilibrium within 60 min, which was an economically favorable requisite, in addition to the local abundance of the raw material. The extent of dye removal increased with increasing initial dye concentration, contact time, pH and temperature, and decreased with increasing ionic strength. On the other hand, stirring speed had no important effect on adsorption process. The adsorption process was found to be endothermic and physical in nature. Four kinetic models, the pseudo-first- and second-order equations, Elovich equation and the intraparticle diffusion models were selected to follow the adsorption process. Kinetic parameters, rate constants, equilibrium adsorption capacities and related correlation coefficients for each kinetic model were calculated and discussed. It was shown that the adsorption of maxilon blue 5G onto sepiolite could be described by the pseudo-second-order equation. The diffusion coefficients were calculated and found to be in the range of $3.625 \times 10^{-8}$ to $12.100 \times 10^{-9}$ cm$^2$/s. Various thermodynamic activation parameters such as enthalpy of sorption $\Delta H^*$, Gibbs energy change $\Delta G^*$ and entropy $\Delta S^*$ were estimated. The positive value of $\Delta H^*$ and $\Delta G^*$ shows the sorption process is endothermic and not spontaneous. The negative value of entropy $\Delta S^*$ shows the decreased randomness at the solid–liquid interface during the sorption of dye ions onto sepiolite particles. In addition, an activation energy of sorption has also been determined based on the pseudo-second-order rate constants. The activation energy of system ($E_a$) was calculated as 19.25 kJ/mol. Sepiolite, an inexpensive and easily available material, could be an alternative for more costly adsorbents used for dye removal in wastewater treatment processes.

*Keywords:* Sepiolite; Dye; Adsorption kinetics; Mechanism

## 1. Introduction

Dyes and pigments represent one of the problematic groups; they are emitted into wastewaters from various industrial branches, mainly from the dye manufacturing and textile finishing and also from food coloring, cosmetics, paper and carpet industries. Synthetic dyes have complex aromatic structures which provide them physico-chemical, thermal and optical properties [1,2]. The presence of dye in water is highly visible and affects water transparency, resulting in reduction of light penetration, and gas solubility in water [3]. Many dyes and pigments are toxic in nature with suspected carcinogenic and mutagenic effects [4] that affect aquatic biota and humans [5]. Removal of such compounds are difficult while many physical and chemical methods including adsorption, coagulation, precipitation, filtration, ozonation, and oxidation have been used for the treatment of dye-containing effluent [6]. There are advantages and disadvantages of various methods of dye removal from wastewaters [7]. Biological oxidation and chemical precipitation process are effective and economic only in the case where the solute concentration are relatively high [8]. But only the adsorption is considered to be superior to other techniques. This is attributed to its low cost, easy availability, simplicity of design, high efficiency, ease of operation, biodegradability, and ability to treat dyes in more concentrated forms [9–11]. The adsorption process provides an attractive alternative for the treatment of contaminated waters, especially, if the sorbent is inexpensive and does not require an additional pre-treatment step before its application [12]. Adsorption has a specific advantage of removing

---

* Corresponding author.
*E-mail addresses:* malkan@balikesir.edu.tr (M. Alkan), mdogan@balikesir.edu.tr (M. Doğan).

1385-8947/$ – see front matter © 2007 Elsevier B.V. All rights reserved.
doi:10.1016/j.cej.2007.07.080

the complete dye molecule, unlike certain removal techniques, which destroy only the dye chromophore leaving the harmful residual moieties (like metals) in the effluent. The environment-friendly, economic feasibility and efficiency criteria limit the practical application of various conventional methods. Amongst the numerous techniques of dye removal, adsorption is a procedure of choice for the removal of dissolved organic compounds from wastewater [13,14].

Activated carbon adsorption has been recognized by United States Environmental Protection Agency (USEPA) as one of the best available control technologies [14,15]. However, the price of activated carbons is relatively high, which limits their usage. At present, there is a growing interest in using other low-cost adsorbents for adsorption. If an adsorbent is inexpensive and ready for use, the adsorption process will be a promising technology. The removal of dyes from industrial wastewaters is currently of great interest. Different adsorbents have been used for removal of dyes [16,17]. This has led many researchers to search for cheaper substitutes such as coal, fly ash, silica gel, wool wastes, agricultural wastes, wood wastes, and clay materials.

Sepiolite forms an important group of clay minerals, which have many industrial, catalytic and environmental applications [18]. Sepiolite is a clay mineral with a unit cell formula $Si_{12}O_{30}Mg_8(OH,F)_4(H_2O)_4 8H_2O$ [19,20], and a general structure formed by an alternation of blocks and tunnels that grow up in the fibre direction. Each block is constructed by two tetrahedral silica sheets enclosing a central magnesia sheet. In some aspects sepiolite is similar to other 2:1 trioctahedral silicates, such as talc, but it has discontinuities and inversions of the silica sheets that give rise to structural tunnels. In the inner blocks, all corners of silica tetrahedra are connected to adjacent blocks, but in outer blocks some of the corners are Si atoms bound to hydroxyls (Si–OH) [21]. Because of their structural morphology, sepiolites have received considerable attention with regard to the adsorption of organics on the clay surfaces and to their use as support for catalysts [18]. These silanol groups at the “external surface” of the silicate [22] are usually accessible to organic species, acting as neutral adsorption sites. In addition to that, some isomorphic substitutions in the tetrahedral sheet of the lattice of the mineral, such as $Al^{3+}$ instead of $Si^{4+}$, form negatively charged adsorption sites. Such sites are occupied by exchangeable cations that compensate for the electrical charge. These characteristics of sepiolite make it a powerful sorbent [23] for neutral organic molecules and organic cations [21].

In the present study, sepiolite have been used as an adsorbent for the removal of maxilon blue 5G from its aqueous solutions. The effects of initial dye concentration, contact time, initial dye solution pH, ionic strength and temperatures on the amount of color removal have been investigated. Also the sorption of maxilon blue 5G at solid–liquid interfaces has been studied extensively at equilibrium. Thermodynamic parameters, the kinetics and the factors controlling the adsorption process were also calculated and discussed. Further the kinetics and the mechanistic steps involved in the sorption process were also evaluated.

Table 1
Some physical properties of sepiolite [24]

| Parameters | Data |
|---|---|
| Color | White |
| Melting temperature (°C) | 1400–1450 |
| Drying temperature (°C) | 40 |
| Reflective index | 1.5 |

Table 2
The chemical composition of sepiolite [24]

| Compounds | Weight (%) |
|---|---|
| $SiO_2$ | 53.47 |
| MgO | 23.55 |
| CaO | 0.71 |
| $Al_2O_3$ | 0.19 |
| $Fe_2O_3$ | 0.16 |
| NiO | 0.43 |
| Weight lossing | 21.49 |

Table 3
Physicochemical properties of sepiolite [24]

| Parameters | Value |
|---|---|
| Surface area ($m^2$/g) | 342 |
| Density (g/cm) | 2.5 |
| Cation exchange capacity (meg/100 g) | 25 |
| pH of solution | 7.8–8.3 |
| Porosity (%) | 50.8 |

## 2. Materials and methods

### 2.1. Materials

Sepiolite sample was obtained from Aktaş Lületaşı Co. (Eskişehir, Turkey). Some physical properties and the chemical composition of the sepiolite found in Eskişehir, Turkey are given in Tables 1 and 2; and some physicochemical properties of it in Table 3 [24]. Maxilon blue 5G [$C_{16}H_{26}N_3O$, MW: 266 g/mol, $\lambda_{max} = 654$ nm] was obtained from Setaş Textile Co. (Bursa, Turkey). The structural form of dye is given in Fig. 1. Sepiolite sample was treated before using in the experiments as follows [25]: the aqueous suspension containing 10 g/L sepiolite was mechanically stirred for 24 h, after waiting for about 2 min the supernatant suspension was filtered through filter paper. The solid sample was dried at 105 °C for 24 h, ground then sieved by 100 μm sieve. The particles under 100 μm was used in further experiments.

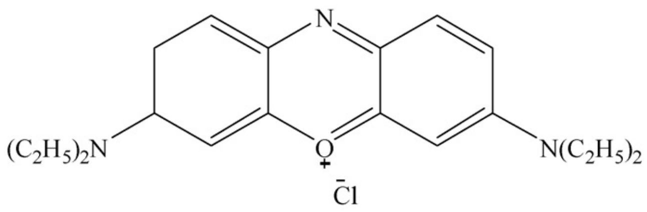

Fig. 1. The structure of maxilon blue 5G.

### 2.2. Experimental procedure

Sorption kinetic experiments were carried out using mechanic stirrer. All of the dye solution was prepared with ultrapure water. Kinetic experiments were carried out by agitating 2 L of dye solution of initial concentration $2 \times 10^{-3}$ mol/L with 5G of sepiolite at a constant agitation speed of 600 rpm, $1 \times 10^{-3}$ mol/L ionic strength (NaCl), 25 °C and pH 9. Agitation was made for 60 min, which is more than sufficient time to reach equilibrium at a constant agitation speed of 600 rpm. Preliminary experiments had shown that the effect of the separation time on the adsorbed amount of dye was negligible. The initial tested concentrations of maxilon blue 5G solution were $1.5 \times 10^{-3}$, $2.0 \times 10^{-3}$ and $2.5 \times 10^{-3}$ mol/L. The effect of pH on the amount of color removal was analyzed in the pH range from 7 to 11. The pH was adjusted using 0.1N NaOH and 0.1N HCl solutions by using a Orion 920A pH-meter with a combined pH electrode. pH-meter was standardized with NBS buffers before every measurement. The effect of ionic strength was investigated at 0.001–0.100 mol/L NaCl salt concentrations. The experiments were carried out at 15, 25, 35 and 45 °C in a constant temperature bath. Two millilitres of samples were drawn at suitable time intervals. The samples were then centrifuged for 15 min at 5000 rpm and the left out concentration in the supernatant solution were analyzed using UV–vis spectrophotometer (Cary 1E UV–vis spectrophotometer, Varian) by monitoring the absorbance changes at a wavelength of maximum absorbance (654 nm). Each experimental run continued until no significant change in the dye concentration was measured. Calibration curves were plotted between absorbance and concentration of the dye solution.

The adsorbed amount of dye at any time $t$, $q_t$, was calculated from the mass balance equation:

$$q_t = (C_0 - C_t)\frac{V}{m} \tag{1}$$

where $C_0$ and $C_t$ are the initial and liquid-phase concentrations at any time $t$ of dye solution (mol/L), respectively; $q_t$ is the dye concentration on adsorbent at any time $t$ (mol/g), $V$ the volume of dye solution (L), and $m$ is the mass of sepiolite sample used (g) [26,27].

## 3. Results and discussion

### 3.1. Adsorption rate

The adsorption kinetic experiments were carried out at different experimental conditions and the results obtained are discussed below.

#### 3.1.1. Effect of contact and equilibrium times

A series of experiments was performed to optimize the adsorption time at an initial dye concentration of $2 \times 10^{-3}$ mol/L. The effect of contact time on adsorption rate of dye is presented in Fig. 2. Effect of contact time for the removal of maxilon blue 5G by sepiolite showed rapid adsorption of dye in the first 5 min and, thereafter, the adsorption rate decreased gradually and the adsorption reached equilibrium in about 60 min. At this point, the adsorbed amount of dye onto sepiolite is in a state of dynamic equilibrium with the amount of the dye desorbing from the adsorbent. The time required to attain this state of equilibrium is termed the equilibrium time, and the adsorbed amount of dye at the equilibrium time reflects the maximum adsorption capacity of the adsorbent under those operating conditions [28,29]. The initial rapid phase may be due to increased number of vacant sites available at the initial stage, as a result there exist increased concentration gradient between adsorbate in solution and adsorbate on the adsorbent surface. This increase in concentration gradient tends to increase in dye sorption rate at initial stages. As time proceeds this concentration gradient gets reduced due to the accumulation of dye particles in the vacant sites, leading to decrease in sorption rate at later stages from 5 to 60 min [8]. The adsorption curves were single, smooth and continuous leading to saturation and indicate the possible mono-layer coverage on the surface of adsorbent by the dye molecules [1]. This was caused by strong attractive forces between the dye molecules and the adsorbent; fast diffusion onto the external surface was followed by fast pore diffusion into the intraparticle matrix to attain rapid equilibrium [16].

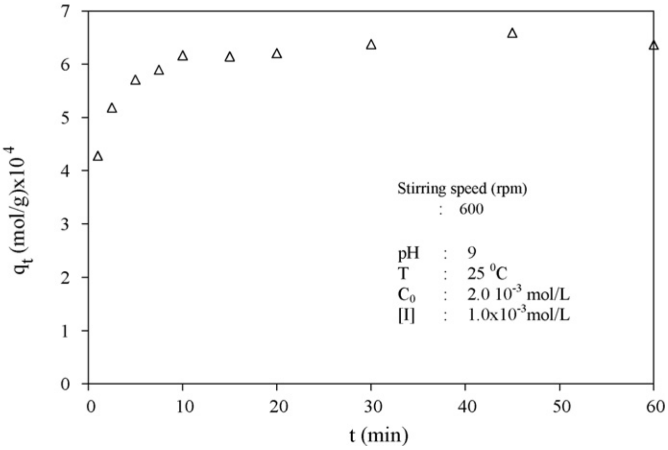

Fig. 2. The effect of contact time to the adsorption rate of maxilon blue 5G on sepiolite.

#### 3.1.2. Effect of stirring speed

The effect of stirring speed on removal rate of maxilon blue 5G with sepiolite was investigated at different stirring speeds such as 200, 400 and 600 rpm. The difference of adsorption rate was insignificant as the stirring speed increases (figure not shown). Similar phenomenas were observed in the kinetic experiments of methyl violet, methylene blue and victoria blue on perlite [25–27], basic brilliant green on modified peat–resin particle [30] and maxilon blue GRL on sepiolite [29].

#### 3.1.3. Effect of initial dye concentration

The initial concentration provides an important driving force to overcome all mass transfer resistances of all molecules between the aqueous and solid phases [29]. Fig. 3 shows the plot of amount of dye adsorbed versus time at different initial dye concentrations. From the figure it was observed that

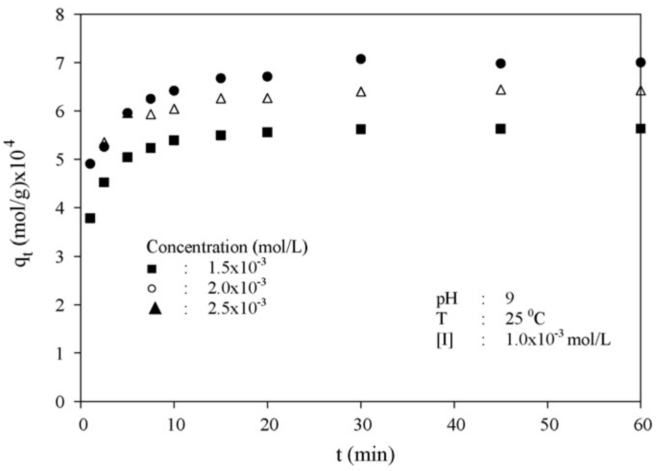

Fig. 3. The effect of initial dye concentration to the adsorption rate of maxilon blue 5G on sepiolite.

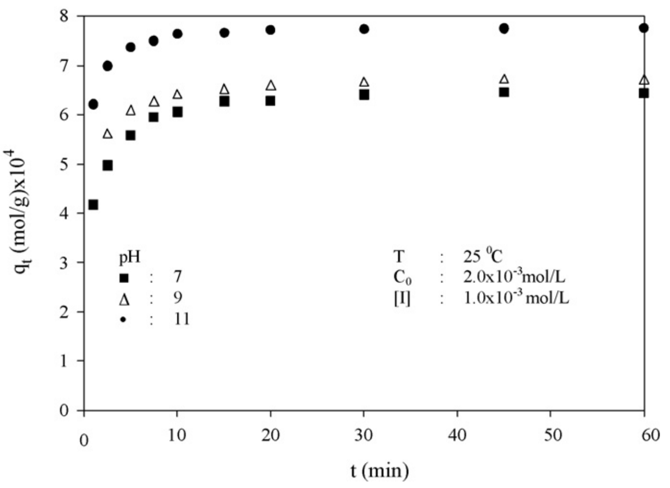

Fig. 4. The effect of pH to the adsorption rate of maxilon blue 5G on sepiolite.

the amount of dye adsorbed gets increased from $5.63 \times 10^{-4}$ to $7.00 \times 10^{-4}$ mol/g for an increase in initial dye concentration from $1.5 \times 10^{-3}$ to $2.5 \times 10^{-3}$ mol/L. Dye removal is highly concentration dependent. The rate of adsorption also increases with the increase in initial dye concentration due to increase in the driving force. In fact, the more concentrated the solution, the better the adsorption. Again, it was observed that at all the initial maxilon blue 5G concentrations, the % removal was very rapid for the first 5 min and thereafter the sorption rate decreased after 30 min and finally reached saturation after 60 min. Furthermore, larger fractions of total amount of adsorbed dye was removed within the first rapid uptake phase, i.e., the first 5 min. This is due to the decrease in flux (concentration gradient) with time due to transfer of solute onto solid phase. The rapid uptake of dye particles at the beginning is due to the occurrence of solute transfer only due to sorbate and sorbent interactions with negligible interference due to solute–solute interactions [31].

### 3.1.4. *Effect of solution pH*

The pH of a solution is of significance for its effect on the adsorbent, as well as on the adsorbate. Both adsorbent and adsorbate may have functional groups that can be protonated or deprotonated to produce different surface charges in solutions at different pH. This results in the electrostatic attraction or repulsion between charged adsorbates and adsorbents [32]. The variation in the removal rate of maxilon blue 5G with respect to pH can be elucidated by considering the surface charge of the adsorbent materials. From Fig. 4, it was observed that the solution pH affects the amount of dye adsorbed. The dye uptake was found to increase with increasing pH and it increases from $6.45 \times 10^{-4}$ to $7.76 \times 10^{-4}$ mol/g for an increase in pH from 7 to 11. Figure demonstrates that the adsorption increases with increasing pH because of the electrostatic attraction between the chromophore groups of dye and the negatively charged sepiolite surface. The higher adsorption of maxilon blue 5G on sepiolite at high pH may result due to the neutralization of the negative sites at the surface of sepiolite. This facilitates diffusion and provides more of the active surface of the adsorbents resulting thereby enhanced adsorption at their surface [29]. Generally, the adsorption capacity increases with increasing pH for cationic dyes, while it decreases with increasing pH for anionic dyes. We had previously shown that sepiolite had a isoelectrical point at pH 6.6 and exhibited positive zeta potential values at the lower pH values from pH 6.6, and negative zeta potential values at the higher pH values from pH 6.6 [33]. As the pH increases from 7 to 11, the number of ionizable sites on sepiolite increases. In this case:

$$\mathrm{SOH} + \mathrm{OH} = \mathrm{SO}^- + \mathrm{H_2O} \qquad (2)$$

With the gradual increase in the pH of the solution, a decrease in the positive charge on the oxide or at solution interface has been observed and the adsorbent surface appears negatively charged due to deprotonation of the adsorbent surface. The removal of dye at higher pH values may be due to the abundance of OH– ions and because of electrostatic attraction between the negatively charged surface of adsorbent and the cationic dye molecules [34]. At higher pH, the surface of sepiolite particles may become negatively charged, which enhances the positively charged maxilon blue 5G cations through electrostatic forces of attraction. In this case, it can be written as follows:

$$\mathrm{SO}^- + \mathrm{Dye}^+ = \mathrm{SO}^- \cdots \mathrm{Dye}^+ \qquad (3)$$

The negatively charged sites favor the adsorption of dye cations due to electrostatic attraction [29]. A similar effect was previously reported by Mall and Upadhyay [35] for methylene blue adsorption on fly ash particles, Doğan and Alkan [26] for methyl violet adsorption on perlite and Doğan et al. for maxilon blue GRL on sepiolite [29].

### 3.1.5. *Effect of ionic strength*

The effect of ionic strength on the adsorption rate is demonstrated in Fig. 5. As seen in Fig. 5, the presence of inorganic salt has significantly influenced the adsorption rate of maxilon blue 5G. For the adsorption of maxilon blue 5G by sepiolite, the adsorption was found to decrease with increasing ionic strength. Since the salt screens the electrostatic interaction of opposite

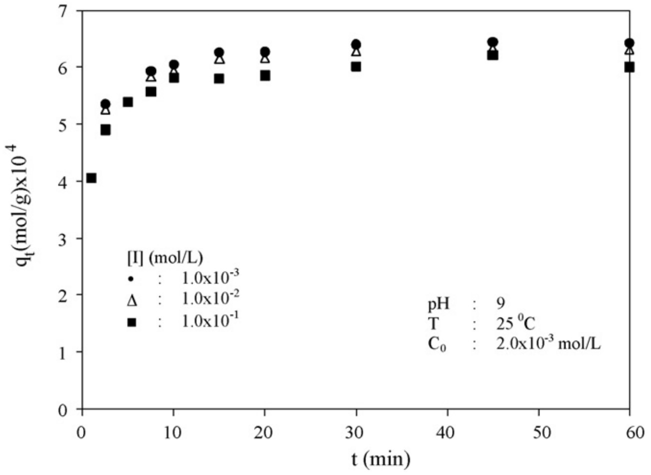

Fig. 5. The effect of ionic strength to the adsorption rate of maxilon blue 5G on sepiolite.

changes of the oxide surface and the dye molecules, the adsorbed amount will decrease with increase of NaCl concentration [36].

### 3.1.6. *Effect of temperature*

The temperature has two major effects on the adsorption process. Increasing the temperature is known to increase the rate of diffusion of the adsorbate molecules across the external boundary layer and in the internal pores of the adsorbent particle, owing to the decrease in the viscosity of the solution. In addition, changing the temperature will change the equilibrium capacity of the adsorbent for a particular adsorbate [29]. Fig. 6 shows the adsorption kinetics of maxilon blue 5G at 15, 25, 35 and 45 °C by plotting the maxilon blue 5G uptake capacity, $q_t$, versus time at the initial maxilon blue 5G concentration of $2 \times 10^{-3}$ mol/L. A larger amount of maxilon blue 5G was removed by sepiolite in the first 5 min of contact time. When the temperature is raised from 15 to 45 °C, the removal of maxilon blue 5G by adsorption onto sepiolite increased from $6.55 \times 10^{-4}$ to $6.95 \times 10^{-4}$ mol/g by increasing the temperature of the solution from 288 to 318 K, indicating that the process is endothermic [11]. As seen in Fig. 6, the adsorbed amount of maxilon blue 5G at equilibrium has increased with increase in temperature. This may be a result of increase in the mobility of the large dye ion with temperature. An increasing number of molecules may also acquire sufficient energy to underground an interaction with active sites at the surface. This kind of temperature dependence of the amount of the dye adsorbed may reflect the increase in the case with which the dye penetrates into sepiolite because of its larger diffusion coefficient. Therefore, it can be said that the adsorption process is endothermic [29].

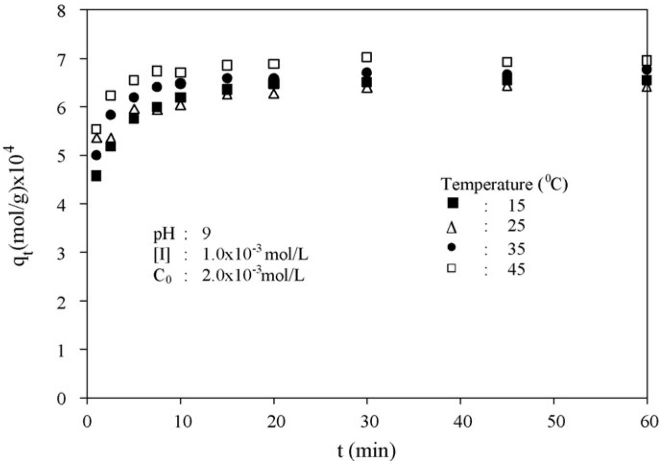

Fig. 6. The effect of temperature to the adsorption rate of maxilon blue 5G on sepiolite.

## 3.2. *Adsorption kinetic models*

Process performance and ultimate cost of a sorption system has been shown to depend upon the effectiveness of process design and efficiency of process operation, which often requires an understanding of the kinetics of uptake or the time dependence of the concentration distribution of the solute in both bulk solution and solid adsorbent [13]. Adsorption is a physiochemical process that involves the mass transfer of a solute (adsorbate) from the fluid phase to the adsorbent surface [37]. A study of kinetics of adsorption is desirable as it provides information about the mechanism of adsorption, which is important for efficiency of the process [38]. The study of adsorption dynamics describes the solute uptake rate. This rate controls the residence time of adsorbate uptake at the solid–solution interface [39]. In order to examine the controlling mechanisms of the adsorption process (such as chemical reaction, diffusion control and mass transfer), several kinetic models were used to test the experimental data. From a system design viewpoint, analysis of adsorption rates using different kinetic equations is very important for practical operations. The kinetics of maxilon blue 5G on sepiolite were analysed using pseudo-first-order, pseudo-second-order, Elovich and intraparticle diffusion kinetic models. The best-fit model was selected based on the linear regression correlation coefficient, $R^2$, values.

### 3.2.1. *The pseudo-first-order model*

The pseudo-first-order kinetic model has been widely used to predict dye adsorption kinetics. The pseudo-first-order kinetic rate equation is expressed as [40]:

$$\frac{\mathrm{d}q_t}{\mathrm{d}t} = k_1(q_\mathrm{e} - q_t) \tag{4}$$

Integrating Eq. (4) and applying the initial conditions $q_t = 0$ at $t = 0$ one has

$$\ln(q_\mathrm{e} - q_t) = \ln q_\mathrm{e} - k_1 t \tag{5}$$

where $q_\mathrm{e}$ is the amount of dye sorbed at equilibrium, mol/g; $q_t$ is the amount of dye sorbed at time $t$, mol/g and $k_1$ is the rate constant of pseudo-first-order sorption, min$^{-1}$. Since $q_t$ reaches a plateau ($q_\mathrm{e}$) at equilibrium, $q_t$ values smaller than the $0.9q_\mathrm{e}$ were used for analysis. The plot of $\ln(q_\mathrm{e} - q_t)$ versus $t$ was used to test the first-order model, and the fitting results are given in Table 4.

Table 4
Kinetic data calculated for adsorption of maxilon blue 5G on sepiolite

| Parameters | | | | | Kinetic models | | | | | | |
|---|---|---|---|---|---|---|---|---|---|---|---|
| Temperature (°C) | Concentration ($\times 10^3$ mol/L) | pH | Stirring speed (rpm) | [*I*] (mol/L) | First-order | Second-order | | | | | Elvoich equation |
| | | | | | $R^2$ | $q_{\mathrm{e,cal}}$ ($\times 10^4$ mol/g) | $q_{\mathrm{e,exp}}$ ($\times 10^4$ mol/g) | $k_2$ (g/(mol min)) | $R^2$ | $h$ ($\times 10^3$ mol/(min g)) | $R^2$ |
| 15 | 2 | 9 | 600 | 0.001 | 0.957 | 6.62 | 6.55 | 2427 | 0.999 | 1.04 | 0.911 |
| 25 | 2 | 9 | 600 | 0.001 | 0.921 | 6.49 | 6.44 | 2969 | 0.999 | 1.23 | 0.918 |
| 35 | 2 | 9 | 600 | 0.001 | 0.709 | 6.79 | 6.77 | 3131 | 0.999 | 1.44 | 0.851 |
| 45 | 2 | 9 | 600 | 0.001 | 0.735 | 6.99 | 6.95 | 4917 | 0.999 | 2.38 | 0.837 |
| 25 | 2 | 7 | 600 | 0.001 | 0.884 | 6.53 | 6.45 | 2199 | 0.999 | 0.916 | 0.893 |
| 25 | 2 | 11 | 600 | 0.001 | 0.903 | 7.79 | 7.76 | 4990 | 0.999 | 3 | 0.809 |
| 25 | 1.5 | 9 | 600 | 0.001 | 0.941 | 5.69 | 5.63 | 3120 | 0.999 | 0.99 | 0.869 |
| 25 | 2.5 | 9 | 600 | 0.001 | 0.931 | 7.11 | 7 | 1656 | 0.999 | 0.812 | 0.946 |
| 25 | 2 | 9 | 600 | 0.01 | 0.921 | 6.37 | 6.33 | 3057 | 0.999 | 1.224 | 0.918 |
| 25 | 2 | 9 | 600 | 0.1 | 0.618 | 6.14 | 6.21 | 2435 | 0.999 | 0.94 | 0.881 |

### 3.2.2. The pseudo-second-order model

The pseudo-second-order kinetic rate equation is expressed as [31]:

$$\frac{\mathrm{d}q_t}{\mathrm{d}t} = k_2(q_\mathrm{e} - q_t)^2 \tag{6}$$

where $k_2$ is the pseudo-second-order rate constant (g/(mol min)). Rearranging the variables in Eq. (6) gives

$$\frac{\mathrm{d}q_t}{(q_\mathrm{e} - q_t)^2} = k_2\,\mathrm{d}t \tag{7}$$

Taking into account, the boundary conditions $t = 0$ to $t = t$ and $q_t = 0$ to $q_t = q_t$, the integrated form of Eq. (7) can be rearranged to obtain the following equation:

$$\frac{1}{(q_\mathrm{e} - q_t)} = \frac{1}{q_\mathrm{e}} + k_2 t \tag{8}$$

Eq. (8) can be rearranged to obtain a linear form:

$$\frac{t}{q_t} = \frac{1}{k_2 q_\mathrm{e}^2} + \frac{t}{q_\mathrm{e}} \tag{9}$$

The initial adsorption rate, $h$ (mol/(g min)) is expressed as

$$h = k_2 q_\mathrm{e}^2 \tag{10}$$

The plot of $(t/q_t)$ versus $t$ of Eq. (9) should give a linear relationship from which $q_\mathrm{e}$ and $k_2$ can be determined from the slope and intercept of the plot, respectively. The calculated $q_\mathrm{e}$, $k_2$, $h$ and the corresponding linear regression correlation coefficient $R^2$ values are summarized in Table 4.

Half-adsorption time, $t_{1/2}$, is defined as the time required for the adsorption to take up half as much sepiolite as its equilibrium value. This time is often used as a measure of the adsorption rate:

$$t_{1/2} = \frac{1}{k_2 q_\mathrm{e}} \tag{11}$$

The values of $t_{1/2}$ determined for the tested parameters are given in Table 4.

### 3.2.3. Elovich equation

In reactions involving chemisorption of adsorbates on a solid surface without desorption of the products, the rate decreases with time due to an increased surface coverage. One of the most useful models for describing such activated adsorption is the Elovich equation [41,42]:

$$\frac{\mathrm{d}q_t}{\mathrm{d}t} = \alpha \exp(-\beta q_t) \tag{12}$$

where $\alpha$ is the initial adsorption rate (mol/(g min)) and $\beta$ is related to the extent of surface coverage and activation energy for chemisorption (g/mol). To simplify the Elvoich equation, it is assumed that $\alpha\beta t \gg 1$ and by applying the boundary conditions $q_t = 0$ at $t = 0$, this equation becomes

$$q_t = \beta \ln(\alpha\beta) + \beta \ln t \tag{13}$$

The testing of experimental data for correspondence with the Elovich equation is carried out by plotting $q_t$ versus $\ln t$. The parameter $\beta$ is obtained from the slope of the line, and the initial

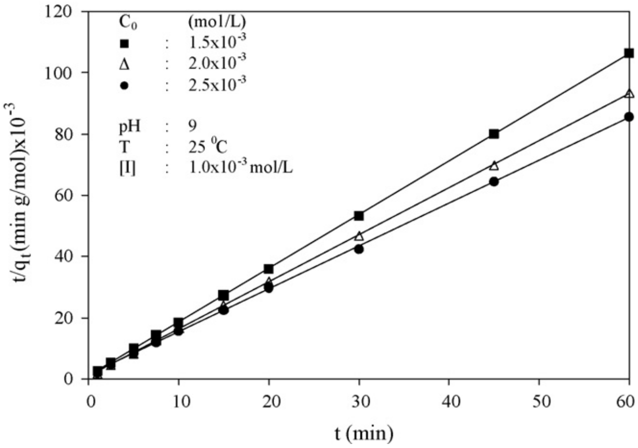

Fig. 7. The plots of $t/q_t$ vs. $t$ for Fig. 3.

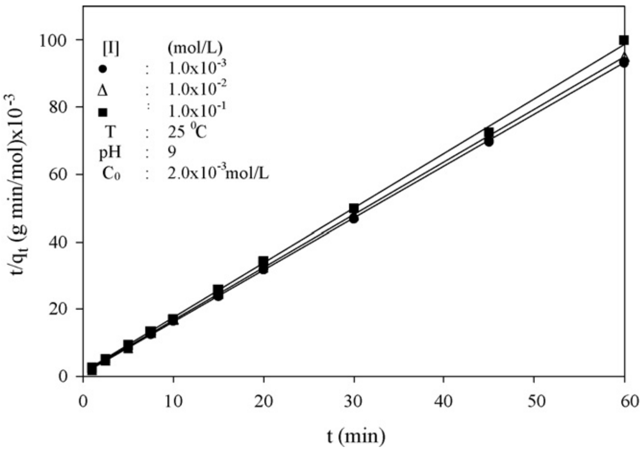

Fig. 9. The plots of $t/q_t$ vs. $t$ for Fig. 5.

rate $\alpha$ is then calculated from intercept of the line. They are also listed in Table 4. The validity of the Elovich equation suggests that chemisorption (chemical reaction) mechanism is likely rate controlling in the present processes [43,44].

The best-fit values of $h$, $q_e$, $\alpha$, $\beta$, rate constants along with correlation coefficients for the pseudo-first-order, pseudo-second-order and Elovich models are shown in Table 4. Since correlation coefficients are closer to unity for the pseudo-second-order kinetic model than those for the other kinetic models, the sorption kinetics can be represented better by the pseudo-second-order kinetics for sepiolite. The calculated adsorption amount at equilibrium ($q_{e,cal}$) shows a difference for first-order model. The $q_{e,cal}$ obtained from the intercepts is inconsistent with the experimental data $q_{e,exp}$. In the second-order model, the $q_{e,cal}$ agrees reasonably well with the experimental data. Thus, the second-order model is more suitable to describe the adsorption kinetics data. This suggests that the adsorption system studied belongs to the second-order kinetic model, based on the assumption that the rate-limiting step may be chemical adsorption or chemisorption. The relationship between $t/q_t$ and $t$ for the second-order adsorption is demonstrated in Figs. 7–10. Similar results were observed in biosorption of dye Remazol Black B, RB2, and PY2 on biomass [45,46], anionic dye adsorption on crosslinked chitosan beads [47,48], polyethylene glycol (PEG) adsorption on zeolite [49], the removal of methylene blue on perlite [27] and the removal of the maxilon blue GRL on sepiolite [29].

### 3.3. Adsorption mechanism

From a mechanistic viewpoint, to interpret the experimental data, it is necessary to identify the steps involved during adsorption, described by external mass transfer (boundary layer diffusion) and intra-particle diffusion [50].

Mass transfer coefficient, $\beta_L$ (m/s) of maxilon blue 5G at the sepiolite–solution interface, were determined by using the following equation [51]:

$$\ln\left(\frac{C_t}{C_0}-\frac{1}{1+mK}\right)=\ln\left(\frac{mK}{1+mK}\right)-\left(\frac{1+mK}{mK}\right)\beta_L S_s t \tag{14}$$

where $K$ is the Langmuir constant (L/g), $m$ the mass of adsorbent (g), and $S_s$ is the surface area of adsorbent (m$^2$/g). A linear graphical relation between $\ln[(C_t/C_0)-1/(1+mK)]$ versus $t$ was

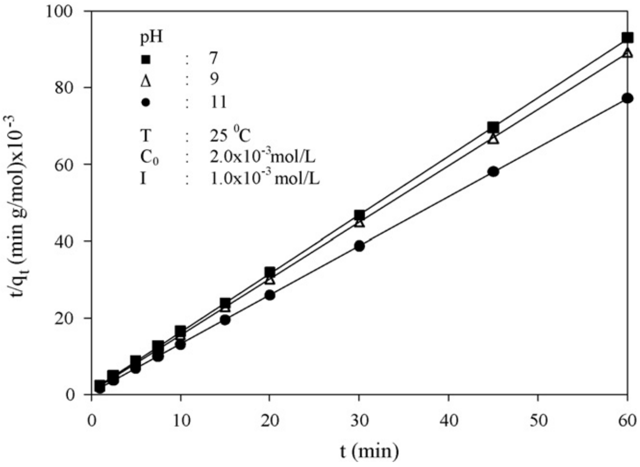

Fig. 8. The plots of $t/q_t$ vs. $t$ for Fig. 4.

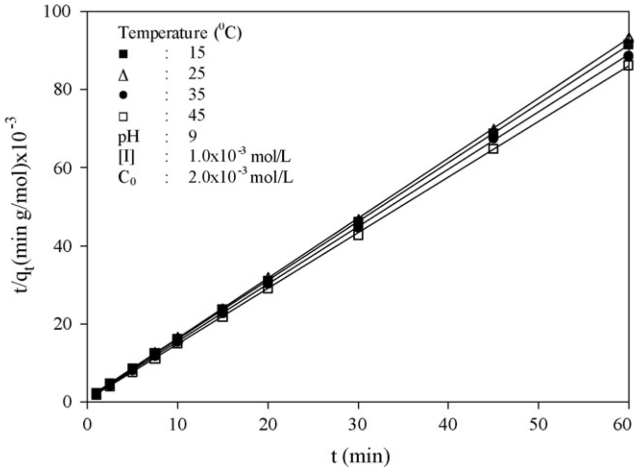

Fig. 10. The plots of $t/q_t$ vs. $t$ for Fig. 6.

not obtained. This result indicates that the model mentioned above for the system is not valid. The values of regression coefficient calculated from equation mentioned above are given in Table 5.

Generally, any sorption process involves three main successive transport steps which are (i) film diffusion, (ii) intraparticle or pore diffusion and (iii) sorption onto interior sites. Among the three steps, the last step is considered negligible as it is assumed to be rapid and hence the rate of sorption should be controlled by either film diffusion or pore diffusion depending on which step is slower [31]. Weber and Morris [52] stated that if intra-particle diffusion is the rate-controlling factor, uptake of the adsorbate varies with the square root of time. Thus, rates of adsorption are usually measured by determining the adsorption capacity of the adsorbent as a function of the square root of time [53]. The mathematical dependence of $q_t$ versus $t^{0.5}$ is obtained if the sorption process is considered to be influenced by diffusion in the spherical particles and convective diffusion in the solution [54,55]. The root time dependence, known also as a Weber–Morris plot [52], may be expressed by the following equation:

$$q_t = k_i\sqrt{t} + C \tag{15}$$

where $k_i$ is the intraparticle diffusion constant. Eq. (15) was applied to the adsorption data, corresponding to the linear portion of the curves. The intraparticle diffusion coefficient for the sorption of maxilon blue 5G was calculated from the slope of the plot of square root of time ($\text{min}^{0.5}$) versus amount of dye adsorbed (mol/g). Previous studies by various researchers showed that the plot between $q_t$ and $t^{0.5}$ represents multi linearity, which characterizes the two or more steps involved in sorption process [29,30,56]. Fig. 11 shows the plot between $q_t$ and $t^{0.5}$ for maxilon blue 5G onto sepiolite particles. From Fig. 11 (other figures not shown), the sorption process tends to be followed by two phases. It was found that an initial linear portion ended with a smooth curve followed by second linear portion. The two phases in the intraparticle diffusion plot suggests that the sorption process proceeds by firstly surface sorption and then the intraparticle diffusion. The initial curved portion of the plot indicates boundary layer effect while the second linear por-

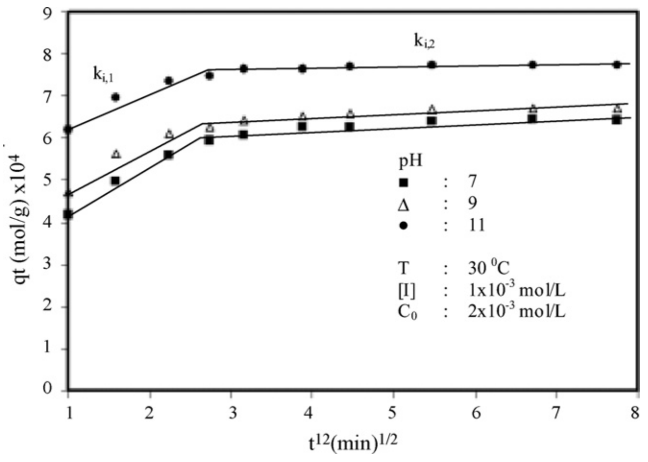

Fig. 11. Intra-particle diffusion plots for different temperatures.

Table 5
Adsorption mechanism and diffusion coefficients of maxilon blue 5G on sepiolite

| Parameters | | | | | Intra-particle diffusion | | | | | Mass transfer, $R^2$ | $t_{1/2}$ (s) |
|---|---|---|---|---|---|---|---|---|---|---|---|
| Temperature (°C) | Concentration ($\times 10^3$ mol/L) | pH | Stirring speed (rpm) | [I] (mol/L) | $k_{i,1}$ ($\times 10^5$) | $R_1^2$ | $k_{i,2}$ ($\times 10^5$) | $R_2^2$ | $D$ ($\times 10^9$ cm$^2$ s$^{-1}$) | | |
| 15 | 2 | 9 | 600 | 0.001 | 8.29 | 0.981 | 6.84 | 0.737 | 4.965 | 0.342 | 37.76 |
| 25 | 2 | 9 | 600 | 0.001 | 8.72 | 0.811 | 6.49 | 0.776 | 5.978 | 0.682 | 31.36 |
| 35 | 2 | 9 | 600 | 0.001 | 7.85 | 0.922 | 5.43 | 0.834 | 6.630 | 0.590 | 28.28 |
| 45 | 2 | 9 | 600 | 0.001 | 6.71 | 0.928 | 4.53 | 0.523 | 10.68 | 0.546 | 17.54 |
| 25 | 2 | 7 | 600 | 0.001 | 10.2 | 0.982 | 7.52 | 0.776 | 4.436 | 0.339 | 42.26 |
| 25 | 2 | 11 | 600 | 0.001 | 26.3 | 0.924 | 6.49 | 0.859 | 12.100 | 0.188 | 15.49 |
| 25 | 1.5 | 9 | 600 | 0.001 | 8.36 | 0.955 | 4.84 | 0.775 | 5.495 | 0.987 | 34.12 |
| 25 | 2.5 | 9 | 600 | 0.001 | 8.11 | 0.986 | 12.2 | 0.725 | 3.625 | 0.641 | 51.72 |
| 25 | 2 | 9 | 600 | 0.010 | 3.93 | 0.811 | 7.37 | 0.776 | 6.044 | 0.499 | 31.02 |
| 25 | 2 | 9 | 600 | 0.100 | 8.61 | 0.932 | 7.13 | 0.619 | 4.728 | 0.354 | 39.65 |

Table 6
Adsorption order, mechanism and diffusion coefficients of some dyes on various adsorbents

| Adsorbents | Reaction order | Adsorbats | Adsorption mechanism | Diffusion coefficients, $D$ ($\times 10^{10}$ cm$^2$/s) | Refs. |
|---|---|---|---|---|---|
| Fly ash | Pseudo-second-order | Methylene blue | Particle diffusion | 20.6 | [8] |
| Biosorbent | Pseudo-first-order | Methylene blue | – | – | [58] |
| Bottom ash | Pseudo-first-order | Quinoline yellow | – | – | [59] |
| Calcined alunite | Pseudo-second-order | Reactive dyes | Mass transfer | – | [60] |
| Bagasse fly ash | Pseudo-second-order | Orange-G, methyl violet | – | – | [61] |
| Activated carbon | First-order | Methylene blue | Intra-particle diffusion | – | [57] |
| Pith | Pseudo-second-order | Basic red 22 | Intra-particle diffusion | – | [31] |
| Wood | – | Astrazone blue | Intra-particle diffusion | 0.006–0.0018 | [54] |
| Wood | – | Telon blue | Intra-particle diffusion | 0.003–0.008 | [54] |
| Perlite | Pseudo-second-order | Methylene blue | Intra-particle diffusion | 24.2–68.7 | [27] |
| Perlite | Pseudo-second-order | Methyl violet | Intra-particle diffusion | 17.4–27.7 | [26] |
| Perlite | Pseudo-second-order | Victoria blue | – | – | [25] |
| Modified peat–resin particle | – | Basic dyes | Intra-particle diffusion | – | [30] |
| Sepiolite | Pseudo-second-order | Maxilon blue GRL | Intra-particle diffusion | 5.16–30.00 | [29] |
| Shale oil ash | – | Reactive dyes | – | 7000–12,700 | [62] |
| Carbon | – | Phenol | – | 901 | [63] |
| Carbon | – | Benzene | – | 80 | [64] |

tion is due to intraparticle or pore diffusion. Since $k_{i,1}$ values for first part of plot are high, this step is not rate limiting step. The slope of second linear portion of the plot has been defined as the intraparticle diffusion parameter $k_{i,2}$ (mol/(g min$^{0.5}$)). On the other hand, the intercept of the plot reflects the boundary layer effect. Values of intercept give an idea about the thickness of boundary layer. Larger the intercept, greater is the contribution of the surface sorption in the rate-limiting step [57]. The calculated intraparticle diffusion coefficient $k_{i,1}$ and $k_{i,2}$ values at different conditions were shown in Table 5. The $k_{i,1}$ and $k_{i,2}$ express diffusion rates of the different stages in the adsorption. At the beginning, the dye was adsorbed by the exterior surface of sepiolite particle, so the adsorption rate was very fast. When the adsorption of the exterior surface reached saturation, the molecular dye entered into the sepiolite particle by the pore within the particle and was adsorbed by the interior surface of the particle. With decrease of the dye concentration in the solution, the diffusion rate became lower and lower, the diffusion processes reached the final equilibrium stage. Therefore, the changes of $k_{i,1}$ and $k_{i,2}$ could be attributed to the adsorption stages of the exterior surface, interior surface and equilibrium, respectively. Therefore, the rate-limiting step in adsorption process is intraparticle diffision due to low $k_{i,2}$ values.

Table 6 shows the adsorption orders and mechanisms of some dyes on various adsorbents from aqueous solutions. As seen in Table 6, similar results were found for basic red 22 on pith, for methylene blue on perlite, for maxilon blue GRL on sepiolite and for methylene blue on fly ash.

The diffusion coefficient largely depends on the surface properties of adsorbents. The diffusion coefficients for the adsorption of maxilon blue 5G on sepiolite particles have been calculated under various conditions by employing the following equation:

$$t_{1/2} = \frac{0.030 r_0^2}{D} \tag{16}$$

where $D$ is the diffusion coefficient with the unit cm$^2$/s; $t_{1/2}$ is the time (s) for half adsorption and $r_0$ is the radius of the adsorbent particle in cm. The value of $r_0$ was calculated as $2.5 \times 10^{-3}$ cm for sepiolite sample. In these calculations, it has been assumed that the solid phase consists of spherical particles with an average radius between the radii corresponding to upper- and lower-size fractions. Table 5 has shown the diffusion coefficients calculated for adsorption of maxilon blue 5G on sepiolite from aqueous solutions. We found that the diffusion coefficients in this study changed in the range of $3.625 \times 10^{-8}$ to $12.1 \times 10^{-9}$ cm$^2$/s under various conditions using Eq. (16). For example, as seen from Table 5, the values of diffusion coefficients increased from $4.965 \times 10^{-8}$ to $12.100 \times 10^{-9}$ cm$^2$/s with change in temperature from 15 to 45 °C, respectively. Comparing to the results in literature (Table 6), our results agree with those of benzene on carbon [63], methyl violet and methylene blue on perlite [26,27], methylene blue on fly ash [8] and maxilon blue GRL on sepiolite [29]. On the other hand, our results are higher than those of astrazone blue and telon blue on wood [53] when they are smaller than those of reactive dyes on shale oil ash [62] and phenol on carbon [63].

### 3.4. Activation parameters

The second-order rate constants listed in Table 4 are used to estimate the activation energy of the maxilon blue 5G adsorption on sepiolite using Arrhenius equation:

$$\ln k_2 = \ln k_0 - \frac{E_a}{R_g T} \tag{17}$$

where $E_a$ is the activation energy (J/mol), $k_2$ the rate constant of sorption (g/(mol s)), $k_0$ is Arrhenius factor, which is the temperature independent factor (g/(mol s)), $R_g$ the gas constant (J/(K mol)), and $T$ is the solution temperature (K).

The slope of plot of $\ln k_2$ versus $1/T$ is used to evaluate $E_a$, which was found to be 19.25 kJ/mol. The magnitude of

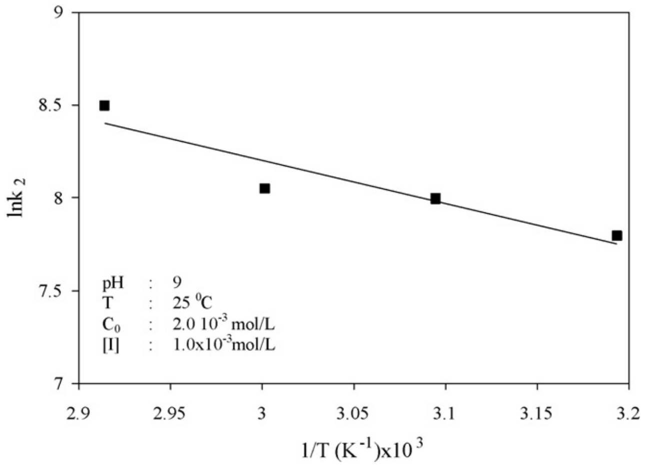

Fig. 12. Arrhenius plot for the adsorption of maxilon blue 5G on sepiolite.

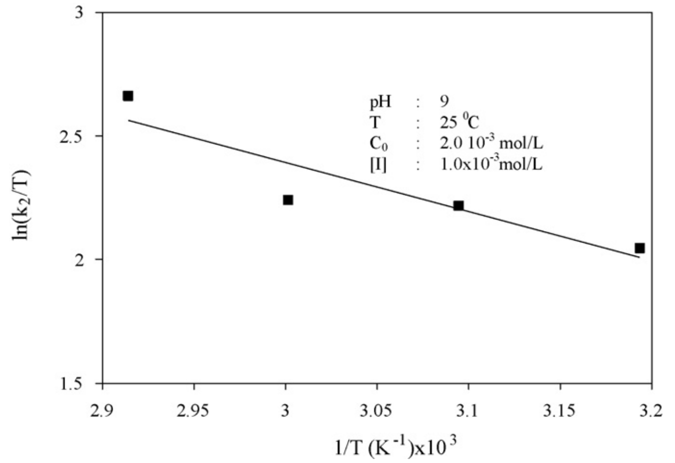

Fig. 13. Plot of ln($k_2/T$) vs. $1/T$ for adsorption of maxilon blue 5G on sepiolite.

activation energy gives an idea about the type of adsorption which is mainly physical or chemical. Low activation energies (5–40 kJ/mol) are characteristics for physisorption, while higher activation energies (40–800 kJ/mol) suggest chemisorption [64]. The result obtained for the adsorption of maxilon blue 5G onto sepiolite indicates that the adsorption has a potential barrier and corresponding to a physisorption (Fig. 12). Therefore, the affinity of maxilon blue 5G for sepiolite may be ascribed to Van der Waals forces, electrostatic attractions or hydrogen bonds between the dye and the surface of the particles. These values are consistent with the values in the literature where the activation energy was found to be 43.0 kJ/mol for the adsorption of Reactive Red 189 on crosslinked chitosan beads [65], 5.6–49.1 kJ/mol for the adsorption of polychlorinated biphenyls on fly ash [66] and 33.96 kJ/mol for the adsorption of maxilon blue GRL on sepiolite [29].

Another aim of this paper is to consider the effect of solution temperature on the transport/kinetic process of dye adsorption. Therefore, the thermodynamic activation parameters of the process such as enthalpy $\Delta H^*$, entropy $\Delta S^*$ and free energy $\Delta G^*$ were determined using the Eyring equation [67]:

$$\ln\left(\frac{k_2}{T}\right) = \ln\left(\frac{k_\mathrm{b}}{h}\right) + \frac{\Delta S*}{R_\mathrm{g}} - \frac{\Delta H*}{R_\mathrm{g} T} \qquad (18)$$

where $k_\mathrm{B}$ is the Boltzmann constant ($1.3807 \times 10^{-23}$ J/K) and $h_\mathrm{P}$ is the Planck constant ($6.6261 \times 10^{-34}$ J s). Fig. 13 shows the plot of ln($k_2/T$) against $1/T$. The result obtained for the change of Gibbs energy are +57.9 kJ/mol at 25 °C. This indicated that the adsorption reaction was not a spontaneous one and that the system gained energy from an external source. The value of the standard enthalpy change (16.35 kJ/mol) indicates that the adsorption is physical in nature involving weak forces of attraction and is also endothermic. At the same time, the low value of $\Delta H^*$ implies that there was loose bonding between the adsorbate molecules and the adsorbent surface [68]. The negative standard entropy change ($\Delta S^*$) value (−162.5 J/(K mol)) corresponds to a decrease in the degree of freedom of the adsorbed species. In this case, the attractions between dye and adsorbent can be given as follows:

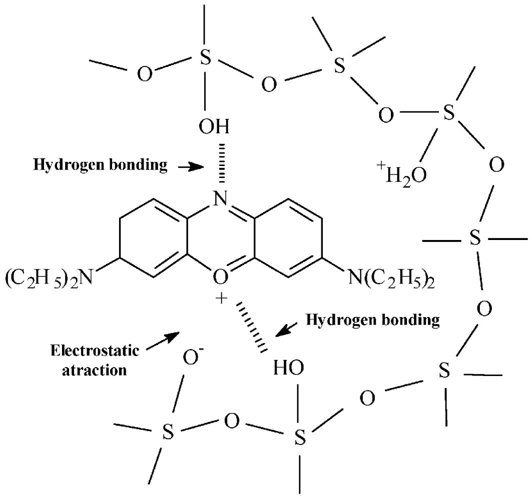

(19)

### 3.5. Conclusions

The present study shows that the sepiolite can be used as an adsorbent for the removal of maxilon blue 5G from its aqueous solutions. The amount of dye sorbed was found to vary with initial dye concentration, contact time, solution pH, ionic strength and temperature. The amount of dye uptake (mol/g) was found to increase with increase in contact time, initial dye concentration, pH and solution temperature, and found to decrease with increase in ionic strength. The results demonstrate a highly significant linear relationship between adsorbed maxilon blue 5G, $t/q_t$, and $t$ in this study with high correlation coefficients. This suggests that the adsorption system studied belongs to the second-order kinetic model, based on the assumption that the rate-limiting step may be chemical adsorption. The dye uptake process was found to be controlled by external mass transfer at earlier stages and by intraparticle diffusion at later stages. Thermodynamic activation parameter shows that the process is endothermic. The positive value of the Gibbs energy change of the adsorption indicates that the adsorption is not spontaneous. The positive value of the enthalpy change of the adsorption shows that the adsorption is an endothermic process. Thus, raising the temperature leads to higher maxilon blue 5G adsorption at equilibrium. Electrostatic attraction and hydrogen bonds are found to be the dominant interactions between maxilon blue 5G and sepiolite surface. The results of this research were compared to the published data in the same field, and found to be in agreement with most of them. The kinetic data may be useful for environmental technologist in designing treatment plants for color removal from wastewaters enriched with maxilon blue 5G. Sepiolite has a high potential to adsorb reactive dyes from aqueous solutions. Therefore, it can be effectively used as an adsorbent for the removal of maxilon blue 5G from wastewaters.

## References

[1] I.D. Mall, V.C. Srivastava, N.K. Agarwal, I.M. Mishra, Chemosphere 61 (2005) 492–501.
[2] P. Janos, H. Buchtova, M. Ryznarova, Water Res. 37 (2003) 4938–4944.
[3] S. Wang, H. Li, J. Hazard. Mater. B126 (2005) 71–77.
[4] G. McKay, M.S. Otterburn, D.A. Aga, Water Air Soil Pollut. 24 (1985) 307–322.
[5] A.R. Gregory, S. Elliot, P. Kluge, J. Appl. Toxicol. 1 (1991) 308–313.
[6] D. Mohan, K.P. Singh, G. Singh, K. Kumar, Ind. Eng. Chem. Res. 41 (2002) 3688–3695.
[7] V.K. Garg, M. Amita, R. Kumar, R. Gupta, Dyes Pigments 63 (2004) 243–250.
[8] K.V. Kumar, A. Kumaran, Biochem. Eng. J. 27 (2005) 83–93.
[9] R. Sanghi, B. Bhattacharya, Color Technol. 118 (2002) 256–269.
[10] V. Meshko, L. Markovska, M. Mincheva, A.E. Rodrigues, Water Res. 35 (2001) 3357–3366.
[11] Y. Bulut, H. Aydın, Desalination 194 (2006) 259–267.
[12] S.B. Wang, Y. Boyjoo, A. Choueib, Z.H. Zhu, Water Res. 39 (2005) 129–138.
[13] B.S. Inbaraj, C.P. Chiu, G.H. Ho, J. Yang, B.H. Chen, J. Hazard. Mater. B137 (2006) 226–234.
[14] R.S. Blackburn, Environ. Sci. Technol. 38 (2004) 4905–4909.
[15] G. Crini, Bioresour. Technol. 97 (9) (2006) 1061–1085.
[16] H. Aydın, G. Baysal, Desalination 196 (2006) 248–259.
[17] S. Wang, Y. Boyjoo, A. Choueib, Chemosphere 60 (2005) 1401–1407.
[18] R.L. Frost, Z. Ding, Thermochim. Acta 397 (2003) 119–128.
[19] K. Brauner, A. Preisinger, Structure and origin of sepiolite, Miner. Petrol. Mitt. 6 (1956) 120–140.
[20] J. Santaren, J. Sanz, E. Ruiz-Hitzky, Clay Miner. 38 (1990) 63–68.
[21] G. Rytwo, D. Tropp, C. Serban, Appl. Clay Sci. 20 (2002) 273–282.
[22] J.L. Alrichs, J.C. Serna, J.M. Serratosa, Clays Clay Miner. 23 (1975) 119–124.
[23] A. Alvarez, Sepiolite: properties and uses. Palygorskite–sepiolite. Occurrences, genesis and uses, Dev. Sedimentol. 37 (1984) (Elsevier, Amsterdam).
[24] M. Alkan, S. Çelikçapa, Ö. Demirbaş, M. Doğan, Dyes Pigments 65 (3) (2005) 251–259.
[25] M. Alkan, M. Doğan, Fresen. Environ. Bull. 12 (5) (2003) 418–425.
[26] M. Doğan, M. Alkan, Chemosphere 50 (2003) 517–528.
[27] M. Doğan, M. Alkan, A. Türkyılmaz, Y. Özdemir, J. Hazard. Mater. B109 (2004) 141–148.
[28] K.R. Ramakrishna, T. Viraraghavan, Water Sci. Technol. 36 (1997) 189.
[29] M. Doğan, M. Alkan, O. Demirbas, Y. Ozdemir, C. Ozmetin, Chem. Eng. J. 124 (2006) 89–101.
[30] Q. Sun, L. Yang, Water Res. 37 (7) (2003) 1535–1544.
[31] Y.S. Ho, G. McKay, Can. J. Chem. Eng. 76 (1998) 822.
[32] Z. Wu, H. Joo, K. Lee, Chem. Eng. J. 112 (2005) 227–236.
[33] M. Alkan, O. Demirbas, M. Doğan, J. Colloid Interf. Sci. 281 (1) (2005) 240–248.
[34] Z. Wu, I.-S. Ahn, C.-H. Lee, J.-H. Kim, Y.G. Shul, K. Lee, Colloids Surf. A: Physicochem. Eng. Aspects 240 (2004) 157–164.
[35] I.D. Mall, S.N. Upadhyay, J. Indian Pulp Paper Technol. Assoc. 7 (1) (1995) 51–57.
[36] N. Tekin, O. Demirbas, M. Alkan, Micropor. Mesopor. Mater. 85 (3) (2005) 340–350.
[37] S.P. Silva, S. Sousa, J. Rodrigues, H. Antunes, J.J. Porter, I. Gonçalves, S.F. Dias, Sep. Purif. Technol. 40 (3) (2004) 309–315.
[38] A.K. Jain, V.K. Gupta, A. Bhatnagar, Suhas, J. Hazard. Mater. B101 (2003) 31–42.
[39] Y. Nacera, B. Aicha, Chem. Eng. J. 119 (2006) 121–125.
[40] S. Lagergren, Ksver Veterskapsakad Handl. 24 (1898) 1–6.
[41] K. Klusacek, R.R. Hudgins, P.L. Silveston, Chem. Eng. Sci. 44 (1989) 2377–2381.
[42] C. Aharoni, S. Sideman, E. Hoffer, Chem. Technol. Biotechnol. 29 (1979) 404–412.
[43] C. Aharoni, F.C. Tompkins, Kinetics of adsorption and desorption and the Elvoich equation, in: D.D. Eley, H. Pines, P.B. Weisz (Eds.), Advances in Catalysis and Related Subjects, vol. 21, Academic Press, New York, 1970, pp. 1–49.
[44] R.L. Tseng, F.C. Wu, R.S. Juang, Carbon 41 (2003) 487–495.
[45] Z. Aksu, S. Tezer, Process Biochem. 36 (2000) 431–439.
[46] Z. Aksu, Biochem. Eng. J. 7 (2001) 79–84.
[47] M.S. Chiou, H.Y. Li, J. Hazard. Mater. 93 (2002) 233–248.
[48] M.S. Chiou, P.Y. Ho, H.Y. Li, Dyes Pigments 60 (2004) 69–84.
[49] C.Y. Chang, W.T. Tsai, C.H. Ing, C.F. Chang, J. Colloid Interf. Sci. 260 (2003) 273–279.
[50] V.K. Gupta, I. Ali, J. Colloid Interf. Sci. 271 (2004) 321–328.
[51] D. Batabyal, A. Sahu, S.K. Chaudhuri, Sep. Technol. 5 (4) (1995) 179–186.
[52] W.J. Weber, J.C. Morris, J. Sanit. Eng. Div. ASCE 89 (SA2) (1963) 31–59.
[53] Y.S. Ho, G. McKay, Process Biochem. 38 (2003) 1047–1061.
[54] G. McKay, V.J.P. Poots, J. Chem. Technol. Biotechnol. 30 (1980) 279–292.
[55] S.J. Allen, G. McKay, K.Y.H. Khader, Environ. Pollut. 56 (1989) 39–50.
[56] R. Sivaraj, C. Namasivayam, K. Kadirvelu, Waste Manage. 21 (2001) 105–110.
[57] N. Kannan, M. Sundaram, Dyes Pigments 51 (2001) 25–40.
[58] E. Rubin, P. Rodriguez, R. Herrero, J. Cremades, I. Barbara, M.E. Sastre de Vicente, J. Chem. Technol. Biotechnol. 80 (2005) 291–298.
[59] V.K. Gupta, I. Ali, V.K. Saini, T. Van Gerven, B. Van der Bruggen, C. Vandecasteele, Ind. Eng. Chem. Res. 44 (10) (2005) 3655–3664.
[60] M. Ozacar, I.A. Sengil, J. Hazard. Mater. 98 (1–3) (2003) 211–224.
[61] I.D. Mall, V.C. Srivastava, N.K. Agarwal, Dyes Pigments 69 (2006) 210–223.
[62] Z. Al-Qodah, Water Res. 34 (17) (2000) 4295–4303.
[63] G. McKay, S.J. Allen, J. Sep. Process. Technol. 4 (3) (1983) 1–7.
[64] H. Nollet, M. Roels, P. Lutgen, P. Van der Meeren, W. Verstraete, Chemosphere 53 (2003) 655–665.
[65] M.S. Chiou, H.Y. Li, Chemosphere 50 (2003) 1095–1105.
[66] C. Maqueda, J.L. Perez-Rodrıguez, L. Lebrato, Fresen. Environ. Bull. 4 (2) (1995) 129–134.
[67] K.J. Laidler, J.M. Meiser, Physical Chemistry, Houghton Mifflin, New York, 1999, p. 852.
[68] D. Singh, Adsorpt. Sci. Technol. 18 (8) (2000) 741–748.